Microchimica Acta (2018) 185: 344
https://doi.org/10.1007/s00604-018-2872-9

ORIGINAL PAPER

Sandwich electrochemical thrombin assay using a glassy carbon electrode modified with nitrogen- and sulfur-doped graphene oxide and gold nanoparticles

Baoshan He[1]

Received: 21 April 2018 / Accepted: 15 June 2018 / Published online: 28 June 2018

Abstract

Graphene oxide doped with nitrogen and sulfur was decorated with gold nanoparticles (AuNP-SN-GO) and applied as a substrate to modify a glassy carbon electrode (GCE). An aptamer against the model protein thrombin was self-assembled on the modified GCE which then was exposed to thrombin. Following aptamer-thrombin interaction, biotin-labeled DNA and aptamer 2 are immobilized on another AuNP-SN-GO hybrid and then are reacted with the thrombin/AuNP-SN-GO/GCE to form a sandwich. The enzyme label horseradish peroxidase (HRP) was then attached to the electrode by biotin–avidin interaction. HRP catalyzes the oxidation of hydroquinone by hydrogen peroxide. This generates a strong electrochemical signal that increases linearly with the logarithm of thrombin concentration in the range from 1.0×10^{-13} M to 1.0×10^{-8} M with a detection limit of 2.5×10^{-14} M (S/$N = 3$). The assay is highly selective. It provides a promising strategy for signal amplification. In our perception, it has a large potential for sensitive and selective detection of analytes for which appropriate aptamers are available.

Keywords Carbon materials · Protein · Aptamer · Signal amplification

Introduction

For protein detection, signal amplification strategies have been widely implanted in electrochemical assay to achieve low detection limit and high sensitivity [1–5]. Specific nanomaterials are often used in electrochemical methods due to their large specific surface area which allows immobilizing more signal molecules at the electrode surface and well electronic conductivity which make the charge transfer to the electrodes become easier [6–9].

Graphene (Gr) is a two-dimensional carbon material composed of single-layer sheets. It possesses excellent conductivity, good thermal and mechanical properties [10–14]. Furthermore, Gr nanosheets have a huge surface-to-volume ratio, which renders them as striking substrate materials when compounded with inorganic substances and conducting polymers for electrochemical sensing. However, electrical conductivity of graphene cannot be completely controlled because it has no bandgap. Furthermore, the aggregation of graphene during the fabrication can dramatically decrease the surface area and thereby lead to a significant decrease in the conductivity [15, 16].

To overcome these limitations, heteroatom doping of B, F, P, N, and S atoms has been applied to enhance the dispersibility and electro-conductivity of graphene. The dopant atoms can tailor electronic band structure and the physicochemical property of graphene and lead to widespread potential applications [17, 18]. For example, N-doping can induce a negative charge with respect to the delocalized sp^2-hybridized carbon framework, resulting in enhanced electron transfer ability as well as improved electrocatalytic activity [19]. While S-doping can change the electronic structure of

Electronic supplementary material The online version of this article (https://doi.org/10.1007/s00604-018-2872-9) contains supplementary material, which is available to authorized users.

✉ Baoshan He
hebaoshan@126.com

[1] School of Food Science and Technology, Henan Key Laboratory of Cereal and Oil Food Safety Inspection and Control, Henan University of Technology, Lianhua Road 100#, Zhengzhou High & New Technology Industries Development Zone, Zhengzhou 450001, Henan Province, People's Republic of China

Gr by means of affecting π electrons in the carbon lattice [20]. Moreover, co-doped Gr by two elements with different electronegativities can give rise to a unique electron distribution and then result in a synergistic effect [21].

Noble metal nanoparticles such as Au, Ag and Pt have been widely used as sensing materials in electrochemical sensors because they not only maximize the availability of nano-sized electroactive surface area for electron transfer but also provide better mass transport of reactants to the electrocatalyst [22–24]. Au nanoparticles (AuNPs) have been recognized as an excellent mediator in the development of electrochemical sensing platform due to their good conductivity and biocompatibility. Furthermore, they can easily introduce bio-elements on electrode by Au-S bond [25, 26]. Due to the large surface area, N, S co-doped Gr oxide (GO) can decorate with a large number of AuNPs via Au-N and Au-S bonds to further enhance the electrical conductivity of GO and immobilize more aptamer via the interaction of Au-S.

GO doped with nitrogen and sulfur was decorated with gold nanoparticles (AuNP-SN-GO) and a novel sandwich-type assay was fabricated using AuNP-SN-GO as the substrate platform and signal carrier for the amplification of electrochemical signal. The application of AuNP-SN-GO not only provided a good deal of active sites for the immobilization of aptamer but also accelerated the electron transfer rate. AuNP-SN-GO have taken the advantages of large specific surface area to immobilize the second aptamer and horseradish peroxidases. With thrombin as model protein, the designed strategy showed high sensitivity and selectivity. The assay also provided a promising tool to construct efficient and rapid electrochemical detection strategy for a variety of biomarkers.

Experimental

Reagents and materials

Thrombin, human serum albumin (HSA), carcinoembryonic antigen (CEA), alpha fetoprotein (AFP), 6-mercapto-1-hexanol (MCH), graphite powder, $(NH_4)_2S_2O_8$, and thiocarbamide were purchased from Aladdin Chemicals Co. Ltd. (Shanghai, China, http://www.aladdin-e.com/). Phosphate buffer (pH 7.0, 0.1 M) was prepared with Na_2HPO_4 and NaH_2PO_4. Graphene oxide (GO) was synthesized by using Hummer's method [27], and AuNPs were prepared according to the protocol reported by Huang et al. [28] The aptamers sequences were designed according to reference [1] and synthesized by Sangon Biotech Co. Ltd. (Shanghai, China, http://www.sangon.com/):

Thrombin aptamer 1: 5′-SH-(CH_2)6-TTTTTTTT TTGGTTGGTGTGGTTGG-3′

Thrombin aptamer 2: 5′-SH-(CH_2)6-GGTTGGTG TGGTTGG-3′

Bio-DNA: 5′-biotin-AGTAGGCGGCGTTATGGTAT TTTTTTTTTTTT-SH-3′

Apparatus

Electrochemical detection was carried out on a CHI660A electrochemical workstation (Chenhua Co., Shanghai, China, http://www.instrument.com.cn/netshow/SH101344/). A modified GCE (3 mm diameter) was applied as working electrode, a platinum wire as counter electrode, and a saturated calomel electrode as reference electrode. The morphological detection was performed on a Hitachi S-4800 scanning electron microscope (SEM, Tokyo, Japan, http://www.hitachi.com/) and a JEM 2100 transmission electron microscope (TEM, JEOL, Tokyo, Japan, http://www.jeol.de/electronoptics-en/index.php).

Preparation of sandwiched electrochemcial detection platform

GCE was firstly treated with 0.3 and 0.05 μm alumina powder, followed by washing with ethanol and water. 1.0 mg AuNP-SN-GO composite was dispersed in 1.0 mL water to obtain a homogeneous suspension (1 mg mL^{-1}). Then, 10 μL AuNP-SN-GO suspension was applied on GCE surface and dried in the air to obtain AuNP-SN-GO/GCE. Subsequently, 8 μL of thiolated aptamer 1 (1×10^{-5} M) was applied on the AuNP-SN-GO/GCE and then incubated at 30 °C for 12 h. Then, 5 μL of 1×10^{-3} M MCH was dropped onto the aptamer 1/AuNP-SN-GO/GCE and incubated for 30 min. Then, thrombin was applied on the electrode and kept at 37 °C for 60 min.

0.1 mg AuNP-SN-GO was added in 50 μL of 1×10^{-5} M thiolated aptamer 2 and incubated at 30 °C for 12 h to form thiolated aptamer 2 modified AuNP-SN-GO. After centrifuged and washed with phosphate buffer, the mixture was added in 50 μL of 2×10^{-6} M biotin and SH group co-modified DNA (Bio-DNA) and incubated at 37 °C for 2 h to get Bio-DNA modified aptamer 2/AuNP-SN-GO hybrid. The mixture was centrifuged and washed with phosphate buffer. Then, 5 μL of 1 mM MCH was mixed with the aptamer 2 modified AuNP-SN-GO and incubated for 30 min. Subsequently, 8 μL of the Bio-DNA modified aptamer 2/AuNP-SN-GO hybrid was dropped on the electrode and incubated at 37 °C and for 80 min. The detection platform is single-use in this work. The preparation process is showed in Scheme 1.

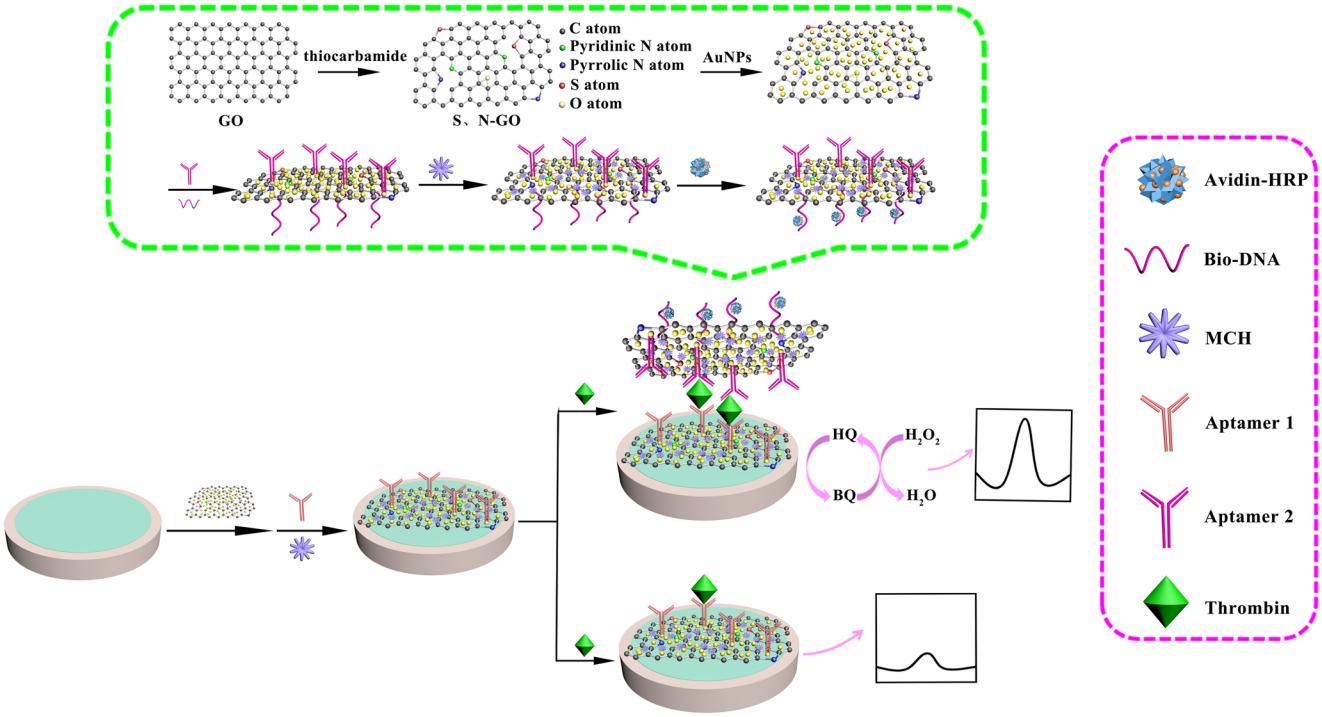

Scheme 1 Schematic diagram of thrombin electrochemical assay

Electrochemical measurement

The electrochemical measurements were performed on a CHI 660D electrochemical workstation (Shanghai CH Instrument, China). The modified working electrode was immersed in a quartz cell at room temperature in 10 mL Phosphate buffer containing 1×10^{-3} M potassium ferricyanide and 1×10^{-4} M KCl and then cyclic voltammetry (CV) was recorded in potential range of −0.2-0.6 V. Differential pulse voltammetry (DPV) was detected in phosphate buffer (pH 7.0) containing 2×10^{-4} M HQ and 2×10^{-4} M H_2O_2 with the pulse amplitude of 0.005 V, pulse width of 0.05 s and the pulse period of 0.2 s. Electrochemical impedance spectroscopy (EIS) measurements were performed in a quartz cell at room temperature in 10 mL phosphate buffer (0.1 M, pH 7.0) containing 5.0×10^{-3} M $[Fe(CN)_6]^{3-/4-}$ and 0.1 M KCl solution from 100 kHz to 0.1 Hz.

Result and discussion

Choice of materials

It is very important to choose suitable material to fabricate a sensing platform because it can amplify the signal and improve its performance. Graphene has been widely used in the fabrication of biosensor due to its unique properties such as superior electric conductivities, high surface areas (theoretical specific surface area of 2620 $m^2\ g^{-1}$) and excellent mechanical strength. However, the aggregation of graphene during the fabrication can dramatically decrease its surface area and thereby lead to a significant decrease in the conductivity. Compared to graphene, GO has good dispersibility in the solution, and keep high specific surface area. On the other hand, heteroatom doping can obviously improve the conductivity of GO. AuNPs are mostly recommended for development of biosensor because they have good conductive ability and can immobilize biomolecular by Au-S bond. In this work, AuNPs modified N, S co-doped GO was used as the substrate platform and signal carrier to fabricate assay for the signal-amplification detection of protein, and it showed good performance.

Characterization of AuNP-SN-GO hybrids

AuNP-SN-GO hybrids were characterized by SEM and TEM. Figure 1a shows the SEM image of the SN-GO hybrid. It displays that the SN-GO hybrid is a layer with some wrinkled and folded regions. The two-dimensional structure of GO is well-retained after doping with N and S. The TEM of SN-GO hybrid in Fig. 1b displays that the SN-GO hybrid is highly transparent with silk-like parts. Figure 1c is the SEM image of the AuNP-SN-GO hybrid. It can be clearly seen that the AuNPs are well dispersed on GO surface, which provides a large surface area and good conductivity. The composition of as-prepared SN-GO hybrids is studied by Energy dispersive

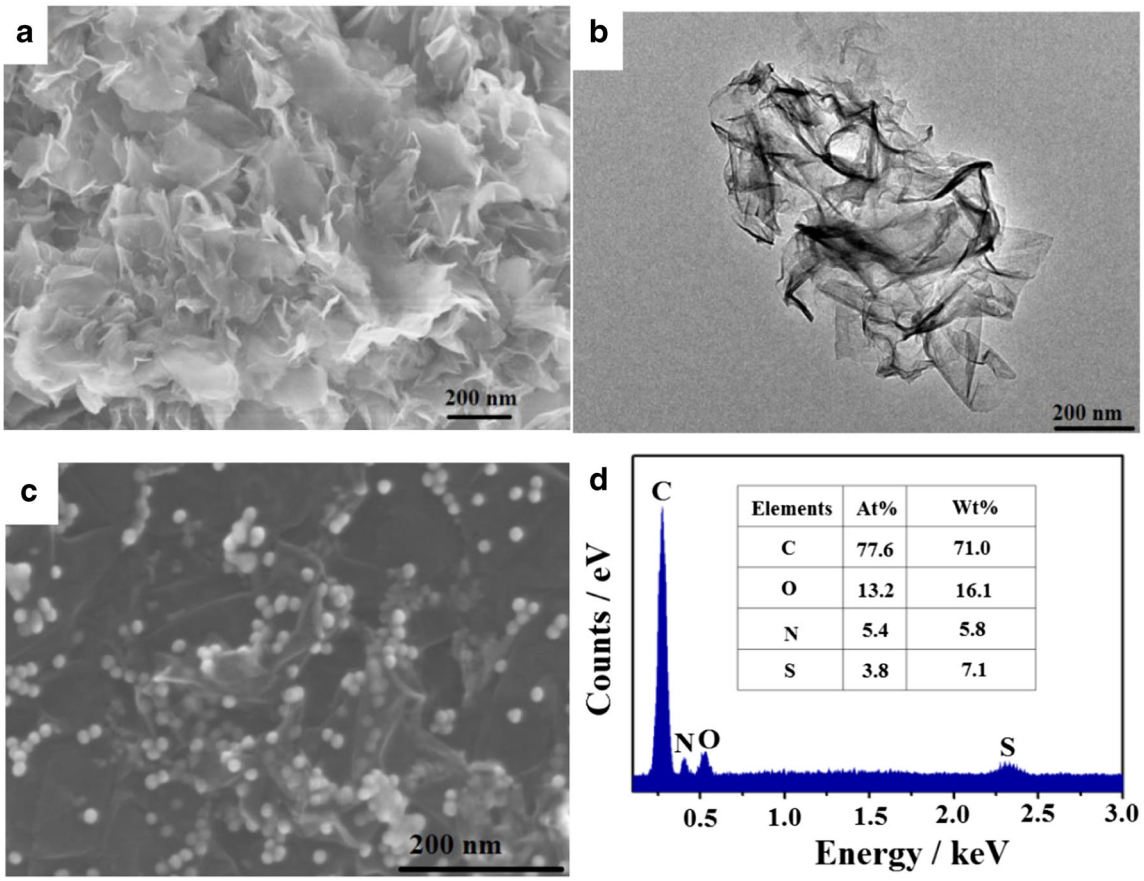

Fig. 1 **a** SEM images of SN-GO; **b** TEM image of SN-GO; **c** SEM images of AuNP-SN-GO hybrid; **d** EDS spectrum of SN-GO

spectrometer (EDS) (Fig. 1d). The results show that there are C, O, N and S elements in the samples. The inset of Fig. 1d displays that the atom content (at%) and weight content (at%) of C, O, N and S elements in the samples. The results of S (3.8 at%) and N (5.4 at%) element contents indicate their contents in the SN-GO sample is minuscule when compared with C, indicating the SN-GO hybrid has been successfully prepared.

Electrochemical characterization

CV and EIS were used to record each fabrication step. During EIS measurements, the impedance spectra includes a semicircle portion and a linear portion. The semicircle portion at higher frequencies displays the electron transfer-limited process, and the linear portion at lower frequencies corresponds to the diffusion-limited process. The semicircle diameter equals the electron transfer resistance. Figure 2a shows bare GCE has a small semicircle at high frequency (curve a). After modified with AuNP-SN-GO, the resistance of GCE is much improved (curve b), demonstrating AuNP-SN-GO has excellent electron transfer ability at interfaces between the electrode surface and the electrolyte solution. The resistance increases after incubation with aptamer 1 (curve c), suggesting that aptamer 1 is linked to AuNP-SN-GO. On account of that the aptamer 1 has mercapto group, which can combine to AuNP-SN-GO by Au-S bond. Afterwards, the resistance of curve d increases, confirming the successful capture of thrombin, and a complex layer blocking electron transfer is generated. Subsequently, the semicircle diameter further increases when the aptamer 2/AuNP-SN-GO/Bio-DNA hybrid is immobilized on the electrode, because the bioactive substances form an additional barrier on the surface of electrode.

As shown in Fig. 2b, the redox peak current density obviously increases comparing with that of bare GCE (curve a) when AuNP-SN-GO is coated on the surface of bare GCE (curve b), because the AuNP-SN-GO with excellent conductivity can effectively accelerate electron transfer. However, the peak current density decreases orderly when the aptamer 1 (curve c), thrombin (curve d) and aptamer 2/AuNP-SN-GO/Bio-DNA hybrid (curve e) are applied on the electrode in accordance with the sequence of modified electrode assembly, because the bioactive substances greatly inhibit the efficiency of electron transfer. Both CV and EIS results convincingly confirm that the designed detection platform is fabricated successfully.

Figure 2c shows the DPVs of various electrodes in the solution containing 2.5×10^{-3} M $[Fe(CN)_6]^{3-/4-}$ and 0.1 M KCl. A weak electrochemical signal can be observed at GCE

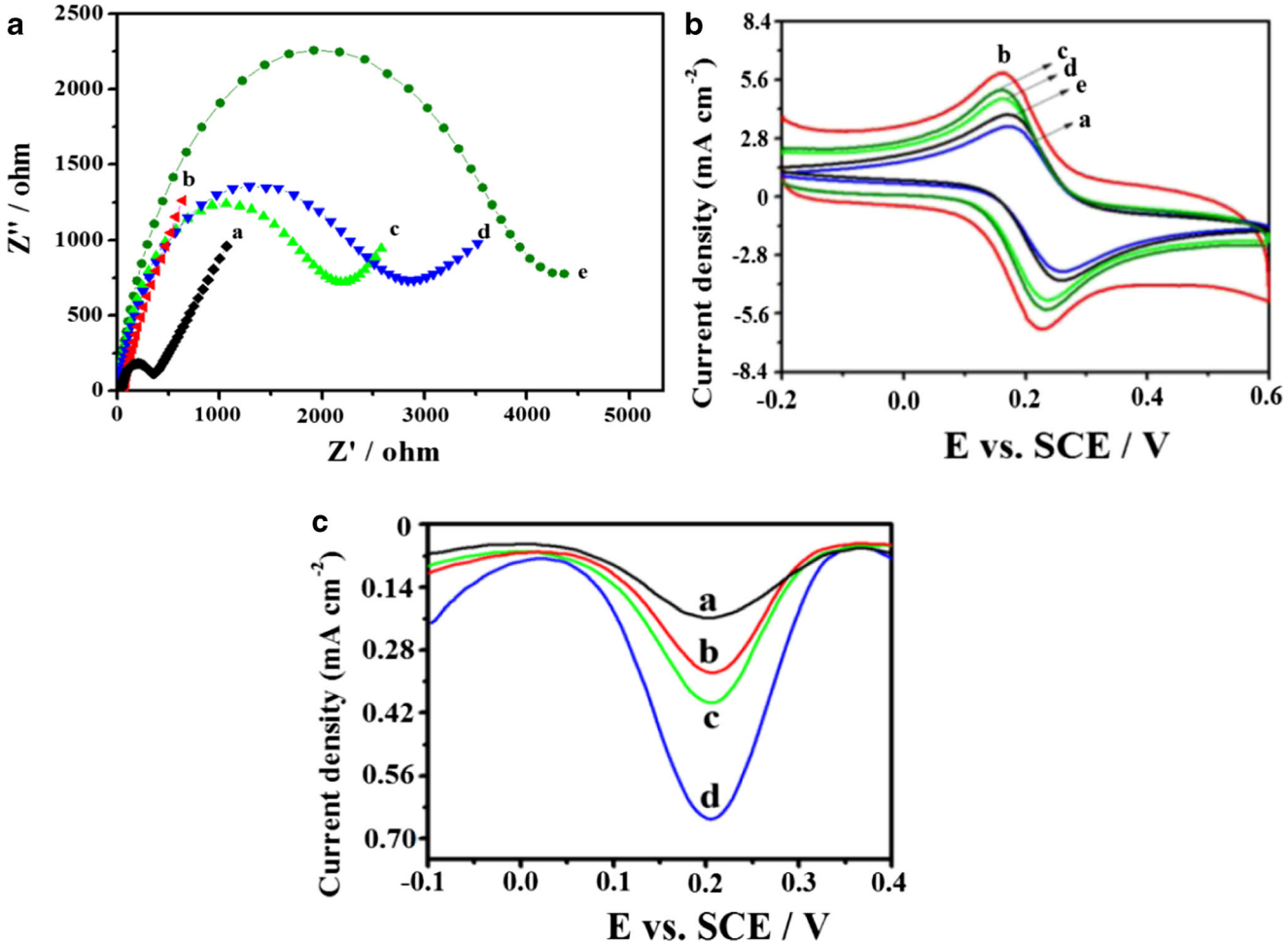

Fig. 2 EIS (**a**) and CVs (**b**) of different electrodes: bare GCE (a), AuNP-SN-GO/GCE (b), aptamer 1/AuNP-SN-GO/GCE (c), thrombin/aptamer 1/AuNP-SN-GO/GCE (d) and GCE/AuNP-SN-GO/aptamer 1/thrombin/aptamer 2/AuNP-SN-GO/Bio-DNA (e); DPV plots of the GCE (a), SN-GO/GCE (b), AuNPs/GCE (c), AuNP-SN-GO/GCE (d)

(a). Nevertheless, we can observe an obviously improved electrochemical response at the SN-GO/GCE (b) and AuNPs/GCE (c), due to good electro-conductivity of SN-GO and AuNPs. While a desired reduction peak appears when AuNP-SN-GO/GCE is used (curve d), testifying that the combination of SN-GO and AuNPs can greatly accelerate electron transfer.

Optimization of method

The following parameters were optimized: (a) AuNPs-SN-Gr loading; (b) Incubation time of thrombin and aptamer1/AuNPs-SN-Gr/GCE hybrid; (c) Incubation time of Bio-DNA and aptamer2/AuNPs-SN-Gr; (d) Incubation time of thrombin and aptamer 2/AuNP-SN-GO/Bio-DNA. Respective data and Figures are given in the Electronic Supplementary Material. The following experimental conditions were found to give best results: (a) optimal loading: 10 μL; (b) Optimal incubation time: 60 min; (c) Optimal incubation time: 120 min; (d) Optimal incubation time: 80 min.

Assay performance

To explore the performance of the assay, a series of concentrations of thrombin were detected under the optimal conditions. The DPV curves were recorded in phosphate buffer (0.1 M, pH 7.4) and the current responses are shown in Fig. 3a. The current response increases gradually with increased thrombin concentration from 1.0×10^{-13} M to 1.0×10^{-8} M. As seen in the inset, the current response and the logarithm of the thrombin concentration exhibits a good linear relationship and the linear regression equation is $y = 6.648\times + 40.336$ ($R^2 = 0.990$), where y is the peak current and x is the logarithm of thrombin concentration (nM). The limit of detection ($S/N = 3$) is 2.5×10^{-14} M. The sensitivity is 7.4×10^5 μA μM^{-1} cm^{-2}. These indicates the designed method can be applied to detect quantitatively thrombin.

A Comparison between this method with others is shown in Table 1. Our assay shows good performance, which may be ascribed to the following factors. Firstly, the AuNP-SN-GO with remarkable electroconductibility can ensure the electron

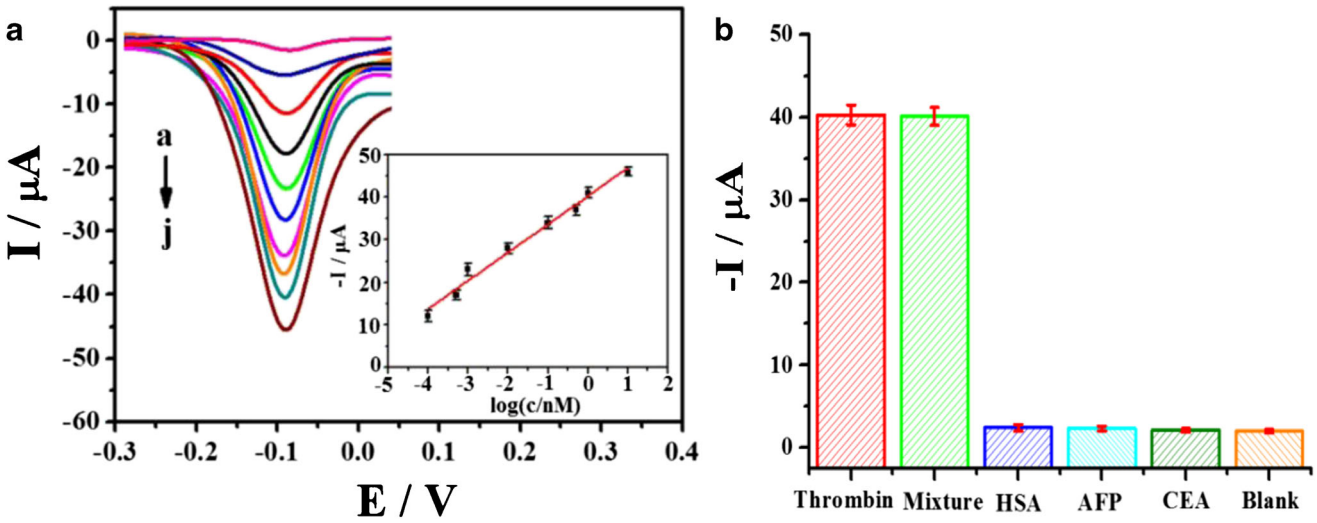

Fig. 3 **a** DPV profiles of different concentrations of thrombin (a-i): 0, 0.000025, 0.0001, 0.0005, 0.001, 0.01, 0.1, 0.5, 1, 10 ($\times 10^{-9}$ M). Inset shows the peak current value versus the logarithmic concentration of thrombin (1×10^{-9} M); **b** The DPV of blank, 1×10^{-6} M CEA, 1×10^{-6} M HSA, 1×10^{-6} M AFP, 1×10^{-6} M thrombin and the mixture of three kinds of these proteins with 1×10^{-9} M

transfer towards the surface of the electrode and the successful conjugation of aptamer. Secondly, AuNP-SN-GO, which shows large specific surface area, possesses well capability for immobilization of more signal molecule leading to higher signal respond.

Specificity, reproducibility and stability

The interference experiments were performed for investigating the specificity of our assay by incubating with interfering protein (including AFP, CEA and HSA). As shown in Fig. 3b, a blank assay is performed in the absence of thrombin, showing a negligible electrochemical response. When the assay is performed in the presence of interfering protein (AFP, CEA and HSA), negligible electrochemical signal is observed which is specially closed to that of the blank. But when the electrochemical response is tested at a comparatively lower concentration (1×10^{-9} M) of thrombin, the result data is a significant increase. Subsequently, the electrode is incubated with 1×10^{-9} M thrombin containing interfering substrates AFP, CEA and HSA, and there are no remarkable changes compared to that of pure 1×10^{-9} M thrombin. The above

Table 1 Comparison between this assay and other reported method for thrombin detection

Material and method	Linear range (M)	Detection limit (M)	Detection time (min)	Sample	Reference
Poly adenine + Electrochemistry	1.0×10^{-13} - 1.0×10^{-8}	3.5×10^{-14}	390	Human serum	[29]
Hyperbranched polyester nanoparticle + Electrochemistry	2.7×10^{-12}-2.7×10^{-7} 1.35×10^{-6} -2.7×10^{-5}	3.1×10^{-14}	135	Human whole blood and serum	[30]
Cu_2O-Au + Electrochemistry	1.0×10^{-12} - 3.0×10^{-8}	3.7×10^{-13}	80	Human serum	[31]
PtNTs@rGO + Electrochemistry	5.0×10^{-14} - 6.0×10^{-8}	1.5×10^{-14}	30	Human serum	[32]
MOF+ Electrochemistry	1.0×10^{-13}-3.0×10^{-8}	6.8×10^{-14}	100	Human serum	[33]
PANI-MWCNTs+ Electrochemistry	1.0×10^{-13}-4.0×10^{-9}	8.0×10^{-14}	–	Human sera	[34]
Magnetic nanospheres + Fluorescence	3.0×10^{-10}-1.11×10^{-8}	9.7×10^{-12}	30	Human serum	[35]
Carbon dots anchored onto silver-decorated polydopamine nanospheres + Electrochemiluminescence	1.0×10^{-15}-5.0×10^{-9}	3.5×10^{-16}	40	–	[36]
GO, AuPtNP + Colorimetry	3.0×10^{-10}-1.0×10^{-7}	1.5×10^{-10}	100	Human serum	[37]
AuPtNP + Electrochemistry	1.0×10^{-13}-2.0×10^{-8}	2.0×10^{-14}	100	Human serum	[38]
CuNPs + Fluorescence	1.0×10^{-8}-8.0×10^{-8}	1.3×10^{-9}	140	–	[39]
MOFs + Fluorescence	5.0×10^{-11}-1.0×10^{-7}	1.5×10^{-11}	90	Plasma	[40]
AuNP-SN-GO+ Electrochemisty	1.0×10^{-13}-1.0×10^{-8}	2.5×10^{-14}	140	Human serum	This work

Table 2 Detection of thrombin in serum samples ($n = 3$)

Samples	Added (1×10^{-12} M)	Detection with ELISA (1×10^{-12} M)	Detection with our method (1×10^{-12} M)	Recovery (%)	RSD (%)
1	0.05	0.049	0.048	96.0	3.2
2	0.5	0.480	0.482	96.4	3.6
3	5	4.920	5.305	106.1	4.3
4	50	53.12	51.90	103.8	4.9

results suggest the assay possessed high specificity for thrombin detection.

The reproducibility of the assay was also evaluated. The electrochemical response was recorded from five parallel-prepared electrode under same experimental conditions. A RSD of 2.4% was obtained for the results, indicating good reproducibility. In addition, the stability of the modified electrode was also studied by keeping it at 4 °C for two weeks, and 90.1% of the initial electrochemical response to 1×10^{-13} M thrombin is obtained, indicating its good stability.

Analysis of serum samples

For evaluating the analytical reliability and potential applications of the assay, recovery test was carried out with the standard addition assay. The serum sample was first performed 10-fold dilution with phosphate buffer. Subsequently, different concentrations of thrombin were spiked into the dilution and then detected with our method. The results are listed in Table 2. The recoveries are 96.0%–106.1% and the RSDs are 3.2%–4.9%. The analytical reliability and application potential of the method were also studied by comparing the assay with ELISA method. The results listed in Table 2 exhibits a good agreement between the ELISA and our method, indicating the assay is potentially applicable to the real biological samples.

Conclusions

A sandwich-type electrochemical assay for the detection of thrombin based on Au nanoparticles decorated N/S codoped graphene was fabricated. AuNP-SN-GO as a substrate platform has a large specific surface area and numerous active sites to capture aptamer and observably accelerate the electron transfer. Additionally, AuNP-SN-GO as a new signal carrier can amplify the electrochemical signal and can easily capture detection aptamer. Compared with the analytical performance of other assays, our method exhibits higher sensitivity and a wider linear range for the detection of protein. Finally, this method is successfully applied to 100-fold diluted serum samples, indicating its potential application in practice. Furthermore, the concept of this method can be expanded to other protein detection (such as immunoglobulin E, carcinoembryonic antigen). However, it should be noted that this sandwich strategy has a major limitation. The fabrication procedure of the sensing platform is somewhat complicated and time-consuming. And there is still much effort needed to use the assay for clinical sample analysis.

Acknowledgements This work was supported by the National Natural Science Foundation of China (Grant No. 61301037), the Henan Science and Technology Cooperation Project (Grant No. 172106000014), the Cultivation Plan for Young Core Teachers in Universities of Henan Province (No. 2017GGJS072) and the Youth Backbone Teacher Training Program of Henan University of Technology.

Compliance with ethical standards The author declares that he has no competing interests.

References

1. Shuai HL, Wu X, Huang KJ (2017) Molybdenum disulfide sphere-based electrochemical aptasensors for protein detection. J Mater Chem B 5:5362–5372
2. Huang KJ, Liu YJ, Zhai QF (2015) Ultrasensitive biosensing platform based on layered vanadium disulfide-graphene composites coupling with tetrahedron-structured DNA probes and exonuclease III assisted signal amplification. J Mater Chem B 3:8180–8187
3. Chen YX, Huang KJ, He LL, Wang YH (2018) Tetrahedral DNA probe coupling with hybridization chain reaction for competitive thrombin aptasensor. Biosens Bioelectron 100:274–281
4. Chen YX, Huang KJ, Niu KX (2018) Recent advances in signal amplification strategy based on oligonucleotide and nanomaterials for microRNA detection-a review. Biosens Bioelectron 99:612–624
5. Shuai HL, Wu X, Huang KJ, Zhai ZB (2017) Ultrasensitive electrochemical biosensing platform based on spherical silicon dioxide/molybdenum selenide nanohybrids and triggered hybridization chain reaction. Biosens Bioelectron 94:616–625
6. Wang YH, Huang KJ, Wu X (2017) Recent advances in transition-metal dichalcogenides based electrochemical biosensors: a review. Biosens Bioelectron 97:305–316
7. Liu YT, Wang HJ, Xiong CY, Yuan YL, Chai YQ, Yuan R (2016) A sensitive electrochemiluminescence immunosensor based on luminophore capped Pd@Au core-shell nanoparticles as signal tracers and ferrocenyl compounds as signal enhancers. Biosens Bioelectron 81:334
8. Xu YH, Wang EK (2012) Electrochemical biosensors based on magnetic micro/nano particles. Electrochim Acta 84:62–73
9. Zaidi SA (2018) Utilization of an environmentally-friendly monomer for an efficient and sustainable adrenaline imprinted electrochemical sensor using grapheme. Electrochim Acta 274:370–377
10. Li SJ, Zhang JC, Li J, Yang HY, Meng JJ, Zhang B (2018) A 3D sandwich structured hybrid of gold nanoparticles decorated MnO_2/

graphene-carbon nanotubes as high performance H_2O_2 sensors. Sensors Actuators B Chem 260:1–11
11. Ensafi AA, Nasr-Esfahani P, Rezaei B (2018) Synthesis of molecularly imprinted polymer on carbon quantum dots as an optical sensor for selective fluorescent determination of promethazine hydrochloride. Sensors Actuators B Chem 257:889–896
12. Kwon SS, Shin JH, Choi J, Nam SW, Park W (2018) Nanotube-on-graphene heterostructures for three-dimensional nano/bio-interface. Sensors Actuators B Chem 254:16
13. Aslan S, Anik Ü (2016) Microbial glucose biosensors based on glassy carbon paste electrodes modified with Gluconobacter Oxydans and graphene oxide or graphene-platinum hybrid nanoparticles. Microchim Acta 183:73–81
14. Chen Z, Hou LQ, Cao Y, Tang YS, Li YF (2018) Gram-scale production of B, N co-doped graphene-like carbon for high performance supercapacitor electrodes. Appl Surf Sci 435:937–944
15. Tepeli Y, Anik U (2016) Preparation, characterization and electrochemical application of graphene-metallic nanocomposites. Electroanal 28:3048
16. Fan HX, Li Y, Wu D, Ma HM, Mao KX, Fan DW, Du B, Li H, Wei Q (2012) Electrochemical bisphenol a sensor based on N-doped graphene sheets. Anal Chim Acta 711:24–28
17. Chen S, Duan JJ, Zheng Y, Chen XM, Du XW, Jaroniec M, Qiao SZ (2015) Ionic liquid-assisted synthesis of N/S-double doped graphene microwires for oxygen evolution and Zn–air batteries. Energ Stor Mater 1:17–24
18. Huang BT, Xiao LL, Dong HF, Zhang XJ, Gan W, Mahboob S, Al-Ghanim KA, Yuan QH, Li YC (2017) Electrochemical sensing platform based on molecularly imprinted polymer decorated N,S co-doped activated graphene for ultrasensitive and selective determination of cyclophosphamide. Talanta 164:601–607
19. Zhang HH, Niu YL, Hu WH (2017) Nitrogen/sulfur-doping of graphene with cysteine as a heteroatom source for oxygen reduction electrocatalysis. J Colloid Interface Sci 505:32
20. Hmar JJL, Majumder T, Dhar S, Mondal SP (2016) Sulfur and nitrogen co-doped graphene quantum dot decorated ZnO nanorod/polymer hybrid flexible device for photosensing applications. Thin Solid Films 612:274–283
21. Tian Y, Mei R, Xue DZ, Zhang X, Peng W (2016) Enhanced electrocatalytic hydrogen evolution in graphene via defect engineering and heteroatoms co-doping. Electrochim Acta 219:781–789
22. Li MR, Wang W, Chen Z, Song ZL, Luo XL (2018) Electrochemical determination of paracetamol based on Au@graphene core-shell nanoparticles doped conducting polymer PEDOT nanocomposite. Sensors Actuators B Chem 260:778–785
23. Li JH, Jiang JB, Xu ZF, Liu MQ, Tang SP, Yang CM, Qian D (2018) Facile synthesis of Ag@Cu_2O heterogeneous nanocrystals decorated N-doped reduced graphene oxide with enhanced electrocatalytic activity for ultrasensitive detection of H_2O_2. Sensors Actuators B Chem 260:529
24. Liu W, Hiekel K, Hübner R, Sun HJ, Ferancove A, Sillanpää M (2018) Pt and Au bimetallic and monometallic nanostructured amperometric sensors for direct detection of hydrogen peroxide: influences of bimetallic effect and silica support. Sensors Actuators B Chem 255:1325–1334
25. Wang YH, Huang KJ, Wu X, Ma YY, Song DL, Du CY, Chang SH (2018) Ultrasensitive supersandwich-type biosensor for enzyme-free amplified microRNA detection based on N-doped graphene/Au nanoparticles and hemin/G-quadruplexes. J Mater Chem B 6: 2134–2142
26. Kalyoncu D, Tepeli Y, Kirgöz UC, Buyraç A, Ül A (2017) Electro-nano diagnostic platforms for simultaneous detection of multiple cancer biomarkers. Electroanal 29:2832–2838
27. Hummers WS, Offeman RE (1958) Preparation of graphitic oxide. J Am Chem Soc 80:1339
28. Chen YX, Huang KJ, Lin F, Fang LX (2017) Ultrasensitive electrochemical sensing platform based on graphene wrapping SnO_2 nanocorals and autonomous cascade DNA duplication strategy. Talanta 175:168
29. Fan TT, Du Y, Yao Y, Wu J, Meng S, Luo JJ, Zhang X, Yang D, Wang CY, Qian Y, Gao FL (2018) Rolling circle amplification triggered poly adenine-gold nanoparticles production for label-free electrochemical detection of thrombin. Sensors Actuators B Chem 266:9
30. Niu YL, Chu ML, Xu P, Meng SS, Zhou Q, Zhao WB, Zhao B, Shen J (2018) An aptasensor based on heparin-mimicking hyperbranched polyester with anti-biofouling interface for sensitive thrombin detection. Biosens Bioelectron 101:174–180
31. Chen S, Liu P, Su K, Li X, Qin Z, Xu W, Chen J, Li CR, Qiu JF (2018) Electrochemical aptasensor for thrombin using co-catalysis of hemin/G-quadruplex DNAzyme and octahedral Cu_2O-Au nanocomposites for signal amplification. Biosens Bioelectron 99:338–345
32. Wu YM, Zou LN, Lei S, Yu Q, Ye BX (2017) Highly sensitive electrochemical thrombin aptasensor based on peptide-enhanced electrocatalysis of hemin/G-quadruplex and nanocomposite as nanocarrier. Biosens Bioelectron 97:317–324
33. Xie SB, Ye JW, Yuan YL, Chai YQ, Yuan R (2015) A multifunctional hemin@metal-organic framework and its application to construct an electrochemical aptasensor for thrombin detection. Nanoscale 7:18232–18238
34. Su ZH, Xu XL, Xu HT, Zhang Y, Li CR, Ma Y, Song DC, Xie QJ (2017) Amperometric thrombin aptasensor using a glassy carbon electrode modified with polyaniline and multiwalled carbon nanotubes tethered with a thiolated aptamer. Microchim Acta 184:1677
35. Wen CY, Bi JH, Wu LL, Zeng JB (2018) Aptamer-functionalized magnetic and fluorescent nanospheres for one-step sensitive detection of thrombin. Microchim Acta 185:77
36. Liu YY, Zhao YH, Fan Q, Khan MS, Li XJ, Zhang Y, Ma HM, Wei Q (2018) Aptamer based electrochemiluminescent thrombin assay using carbon dots anchored onto silver-decorated polydopamine nanospheres. Microchim Acta 185:85
37. Wang L, Yang W, Li TF, Li D, Cui ZM, Wang Y, Ji SL, Song QX, Shu C, Ding L (2017) Colorimetric determination of thrombin by exploiting a triple enzyme-mimetic activity and dual-aptamer strategy. Microchim Acta 184:3145–3151
38. Wang XY, Sun DP, Tong YL, Zhong YS, Chen ZG (2017) A voltammetric aptamer-based thrombin biosensor exploiting signal amplification via synergetic catalysis by DNAzyme and enzyme decorated AuPd nanoparticles on a poly(o-phenylenediamine) support. Microchim Acta 184:1791–1799
39. Cao Y, Wang ZH, Cao JP, Mao XX, Chen GF, Zhao J (2017) A general protein aptasensing strategy based on untemplated nucleic acid elongation and the use of fluorescent copper nanoparticles: application to the detection of thrombin and the vascular endothelial growth factor. Microchim Acta 184:3697–3704
40. He JC, Li GK, Hu YL (2017) Aptamer-involved fluorescence amplification strategy facilitated by directional enzymatic hydrolysis for bioassays based on a metal-organic framework platform: highly selective and sensitive determination of thrombin and oxytetracycline. Microchim Acta 184:2365